

# Frequency-selective response of periodically forced coupled FHN models *via* system size multi-resonance

Gang Zhao, Zhonghuai Hou\* and Houwen Xin\*

Department of Chemical Physics, University of Science and Technology of China, Hefei Anhui, 230026, People's Republic of China

Received 19th May 2005, Accepted 30th August 2005  
First published as an Advance Article on the web 8th September 2005

We consider system of globally coupled FitzHugh–Nagumo (FHN) models; each element is subjected to a subthreshold periodic signal and independent Gaussian white noise. With the variation of the system size, the spike train of the mean field of the system fires according to the period of the subthreshold external signal or to the interior time scale of the FHN model. The influence of the coupling strength is also investigated. It only influences the response of the mean field to external signal. If two external signals are injected to the system simultaneously, the least-common-multiple periods or other common multiples may be selected by different system sizes.

Constructive effects of noise in nonlinear dynamical systems have been widely established in various systems. These effects include stochastic resonance (SR)<sup>1</sup> or coherence resonance (CR),<sup>2</sup> noise-enhanced phase locking,<sup>3</sup> noise-induced transition,<sup>4</sup> and noise-sustained patterns in spatially extended systems,<sup>5</sup> to list just a few. SR is well-known for the resonant noise amplitude at which the response of a system to a periodic signal is maximally ordered, and CR refers to a situation where the order of the response of an excitable system shows a maximum at a certain optimal noise amplitude in the absence of external signals. Of particular interest is the phenomenon of SR or CR in neural systems<sup>6</sup> that have been demonstrated in several experiments. The response to stimuli of the sensory neurons in the tailfans of crayfish,<sup>7</sup> in the cercal system of crickets,<sup>8</sup> and in rat skin<sup>9</sup> shows typical SR signature: the signal-to-noise ratio (SNR) increases with increasing noise amplitude which is added externally, reaches a maximum and decreases when further increasing the noise amplitude. It is more interesting that SR or CR not only takes place in excitable neurons but also in the networks of mammalian brain,<sup>10</sup> in the coherence between the spinal and the cortical neurons in the somatosensory system of an anaesthetized cat,<sup>11</sup> and even in the feeding behavior of a paddlefish.<sup>12</sup>

Classical SR of bistable systems are understood in the context of time-scale matching between the signal and noise induced hopping which depends on the noise amplitude.<sup>13</sup> In addition, in bistable systems, this time-scale matching mechanism of SR also holds in the numerical simulations of the excitable neurons.<sup>14</sup> In the case of CR where the external signal is absent, the excitable system has an intrinsic period that characterizes the temporal behavior of the system. Certain optimal noise amplitude could induce spikes of maximal coherence according to the time-scale of the excitable system,<sup>15</sup> which includes an excitatory and a refractory part. To achieve resonance by these mechanisms, suitable noise amplitude is needed. The requirement for a certain optimal noise amplitude hindered the promising applications of SR or CR in neural systems since it is more difficult to tune noise amplitude directly in nature than in experiments. However, later research pointed out that embedding one element into an array<sup>16</sup> or a network<sup>17</sup> of elements with different coupling strength, different coupling strategy,<sup>18</sup> different topological structure, would remarkably

enhance the effects of SR or CR and broaden the resonant scope of noise amplitude.

To employ SR or CR, another mechanism for adapting to the uncontrollable noise amplitude is the so-called system size resonance,<sup>19</sup> where the effective noise amplitude of a system of coupled elements is inversely proportional to the system size. Pikovsky *et al.*<sup>19a</sup> demonstrated in a system of coupled bistable overdamped oscillators and in the 2-D nearest neighbor Ising model that when other parameters are fixed, the response of the mean field to a periodic forcing can have a maximum at a certain system size. They conjectured in their paper that the mechanism of system size resonance might be employed by neuronal dynamics to achieve the maximal sensitivity, and by changing the coupling strength or connectivity, a neuronal system can tune itself to signals with different frequencies. Toral *et al.*<sup>19b</sup> extended the system size resonance in the coupled FHN models by finding the system size coherent resonance, where in the absence of external forcing the noisy excitable systems pulse on average with a regularity which is optimal for a specific value of the system size. Note that the phenomenon of system size resonance differs from array-enhanced SR in that the system size has a resonant behavior with regard to the coherence of the output.

In the present paper, we show that frequency-selective response is realized *via* system size multi-resonance when considering system of coupled excitable systems, in which each element is subjected to a sub-threshold periodic signal and independent Gaussian white noise. We choose the FHN model as an example because it provides a simple description of the dynamics of a large class of neurons. The equations are<sup>20,21</sup>

$$\dot{x}_i = \frac{1}{\varepsilon} \left( x_i - \frac{1}{3} x_i^3 - y_i \right) + \frac{K}{N} \sum_{j=1}^N (x_j - x_i) + D \xi_i(t) \quad (1)$$

$$\dot{y}_i = x_i + a + A \sin \left( \frac{2\pi}{T_c} t \right) \quad (2)$$

Here  $\xi_i(t)$  is a Gaussian white noise with zero mean and unit variance *i.e.*  $\langle \xi_i(t) \rangle = 0$  and  $\langle \xi_i(t) \xi_j(t') \rangle = \delta_{ij} \delta(t - t')$ ;  $D$  denotes the noise intensity,  $K$  is the coupling strength, and  $N$  is the number of elements in the system.

It is well-known that if  $a > 1$ , the single FHN model stays at a stable fixed point which is excitable. For  $a < 1$ , a stable limit cycle is created through a supercritical Hopf bifurcation, which changes from small amplitude quasi-harmonic oscillation to spikes abruptly through canard explosion. We fix  $a = 1.01$ ,  $\varepsilon = 0.1$ , hence the elements in the system are excitable. The amplitude of the periodic signal is set to be sub-threshold, namely, the signal alone is not capable of triggering spikes. To avoid being masked by the intrinsic period of the self-spiking behavior on the oscillatory side of the bifurcation point, the signal period is set to be larger than the intrinsic one. For the collective behavior of the system, we investigate the mean field  $X(t) = \frac{1}{N} \sum_{i=1}^N x_i(t)$ . The system is numerically integrated by the explicit Euler–Maruyama<sup>22</sup> algorithm with a time step of 0.005. To quantify the coherence in the output, we adopt the commonly used coefficient of variance (CV) of the inter-spike intervals (ISI), which is defined as

$$R = \frac{\sqrt{\langle T^2 \rangle - \langle T \rangle^2}}{\langle T \rangle},$$

where  $T$  is the series of inter-spike intervals. A spike is defined if a certain threshold of the mean-field voltage variable  $X(t)$  is exceeded from below.

We show in Fig. 1a  $R$  of the mean field  $X$  as a function of the system size  $N$ . An interesting bimodal shape which could be called system size bi-resonance appears. The parameters are  $K = 10$ ,  $D = 1$ ,  $A = 0.09$ ,  $T_e = 9$ . We mark those local extrema

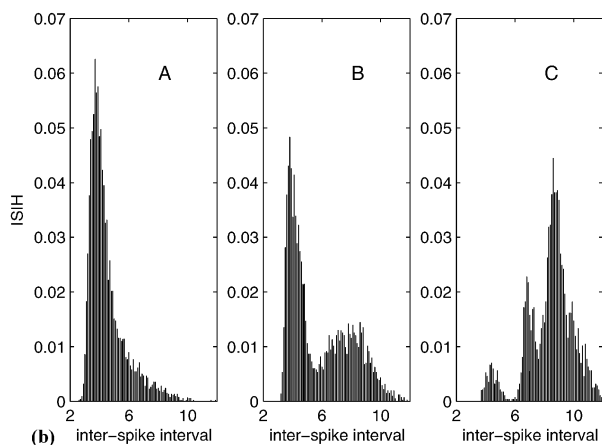
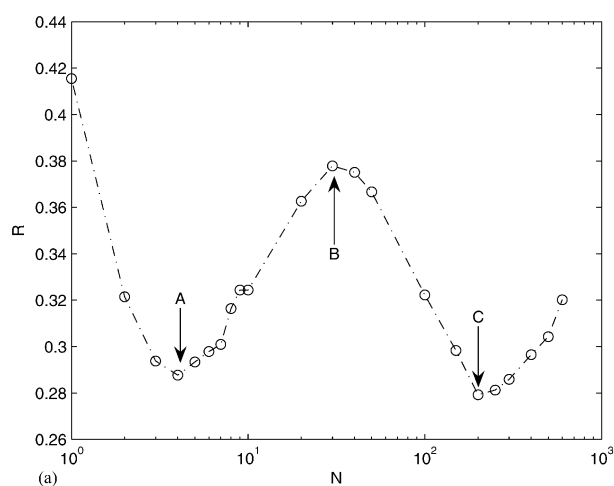


**Fig. 1** (a) System size bi-resonance of globally coupled FHN models. Parameters are  $K = 10$ ,  $D = 1$ ,  $A = 0.09$ ,  $T_e = 9$ . Marked points are:  $N = 5$  (A), 30 (B), 260 (C). (b) The ISIH corresponding to those marked points in (a). The threshold for identifying a spike is 1.0.

as A ( $N = 5$ ), B ( $N = 30$ ) and C ( $N = 260$ ). The corresponding ISI histograms (ISIH) of the mean field are shown in Fig. 1b. When the system size is large ( $N = 260$ ), the mean field fires according to the external signal period  $T_e = 9$ . For small system size ( $N = 5$ ), the mean field fires autonomously according to the self-spiking period of the model  $T_i = 4$ . With intermediate system size ( $N = 30$ ), the firing pattern is a hybrid of  $T_i = 4$  and  $T_e = 9$ . The mean field responds differently due to the variation of the size of the system. Therefore, the frequency-selective response is realized *via* the system size bi-resonance. We have also done simulations for different signal periods. If signal periods  $T_e$  are larger than but close to  $T_i$ , the bimodal shape and the effect of frequency-selective response are not distinct due to the small difference between  $T_e$  and  $T_i$ . The two minima become intermixed to give rise to a broader resonant scope of  $N$ . For larger signal periods, the bimodal shape and the effect of frequency-selective response are strong.

To understand the above phenomena, let us consider the main idea of system size resonance. Coupling a number of elements into the system gives rise to an effective noise amplitude of  $D/\sqrt{N}$  on the mean field, whose dynamics maintains the main features of the couple-free element, which is in<sup>19a</sup> bistability and in<sup>19b</sup> excitability. Following the line, we try to understand the system size bi-resonance by investigating a single periodically forced FHN model. To compare, we numerically integrate eqns (1) and (2) with  $K = 0$  and investigate  $R$  and ISIH. The curve of  $R$  of the output  $x(t)$  vs.  $D$  is shown in Fig. 2a, and the corresponding ISIH of those local extrema marked as A, B, and C are shown in Fig. 2b. The bimodal shape and the effect of frequency-selective response are the

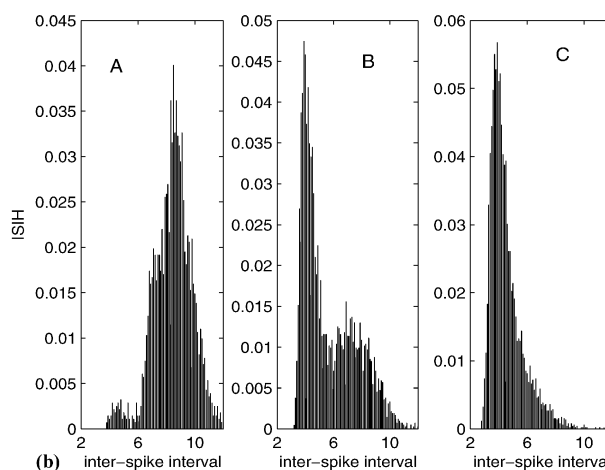
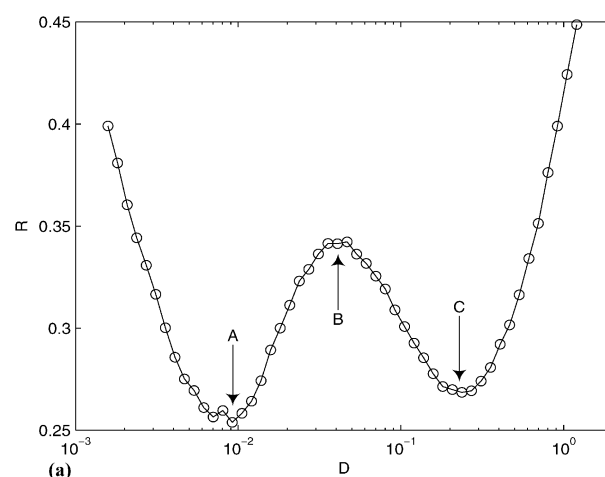


**Fig. 2** (a) The bimodal shape in a single FHN model. Parameters are  $A = 0.09$ ,  $T_e = 9$ . (b) ISIH of the marked points in (a). The threshold for identifying a spike is 1.0.

same as in Fig. 1. The bimodal shape and the effective frequency-selective response of a single FHN model can be understood as following. With the presence of the subthreshold signal, small noise can help the signal surpass the excitable threshold and induce spikes; this is the typical situation of stochastic resonance in threshold systems. The spike train may be organized according to the external signal period ( $T_e$ ) if  $T_e > T_i$  or according to the self-spiking period ( $T_i$ ) if  $T_e < T_i$ , because the FHN model would not respond to stimuli during its refractory period. Further increasing noise amplitude, noise alone could induce spikes; the spike train is now organized according to the intrinsic time-scale ( $T_i$ ) of the excitable system.

When coupled together, the mean field of the system would behave like a 'single' model which is subjected to subthreshold signal and noise with an effective noise amplitude of  $D/\sqrt{N}$ . With the variation of  $N$ , the effective noise amplitude is varied. Therefore, the bimodal shape and the effect of frequency-selective response of the mean field are natural consequences in the context of the above discussion.

To get a more complete knowledge of the system size bi-resonance, we have done simulations to investigate the influence of the coupling strength  $K$ . Results of a detailed scan are shown in Fig. 3. Interestingly, the two minima corresponding to external period and internal time-scale, respectively, behave differently. With the increase of  $K$ , the resonant size that corresponds to external period becomes smaller while the other resonant size that corresponds to internal time scale keeps

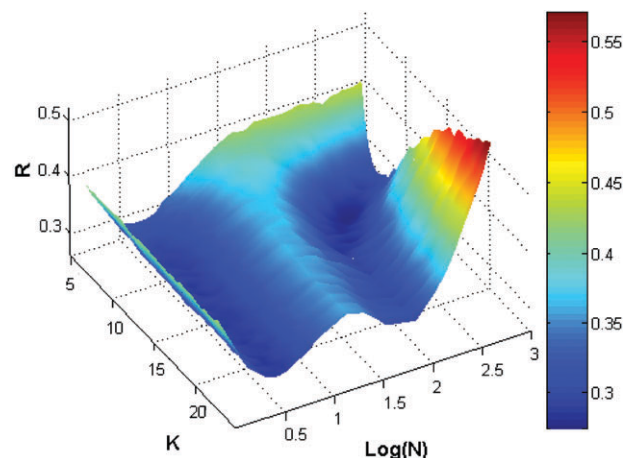


**Fig. 3** (a)  $R$  as a function of  $K$  and  $N$ . Parameters are  $D = 1$ ,  $A = 0.09$ ,  $T_e = 9$ .

constant. Therefore, there is a matching relation between  $K$  and  $N$  to get best response to external signal, however,  $K$  does not influence the response of the system to the internal time-scale.

From the above discussion, one may naturally ask whether it is possible to achieve system size multi-resonance and frequency-selective response in the case of multi-frequency external signal. We have also performed some simulations about

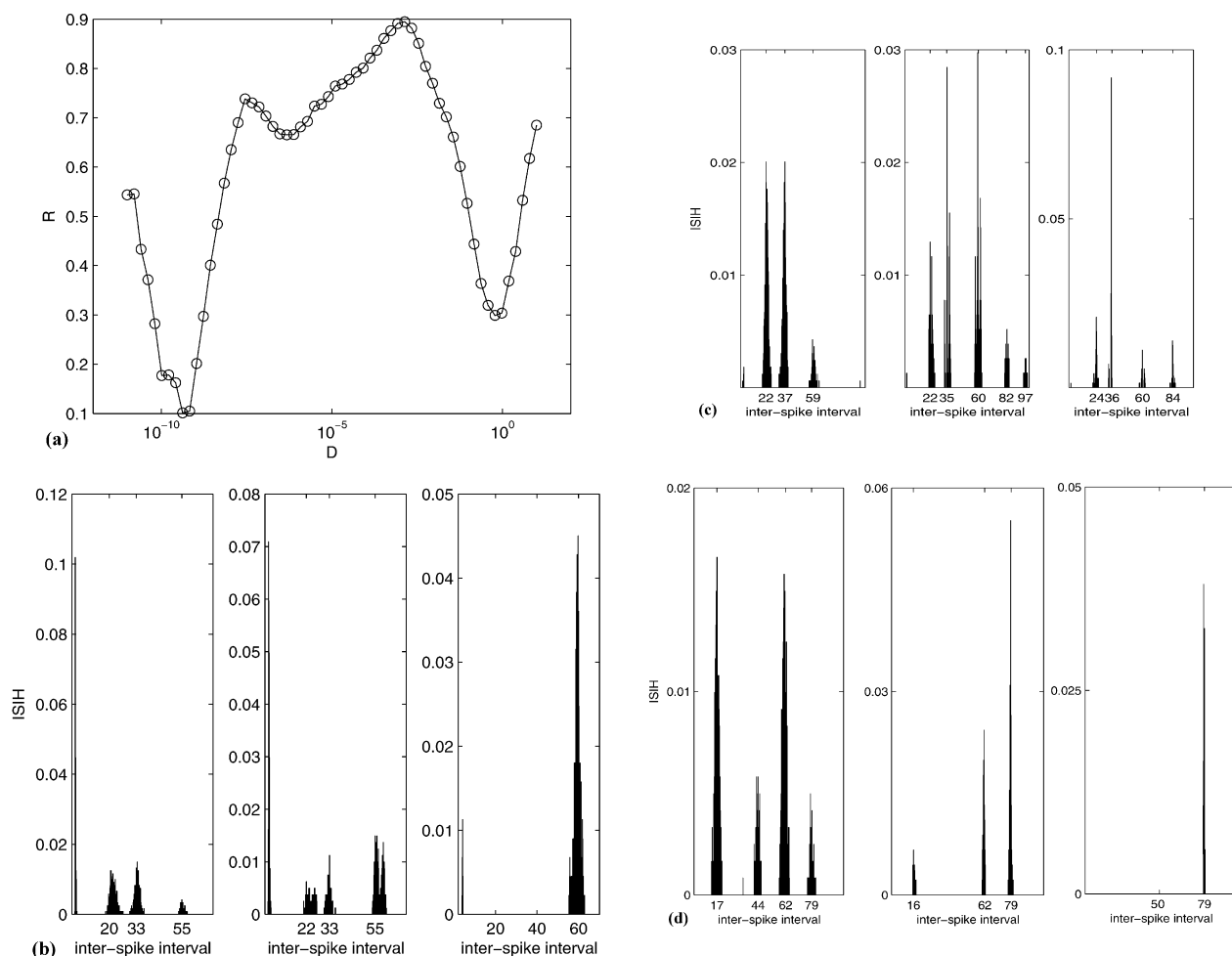


**Fig. 4** (a)  $R$  as a function of  $D$  in a single FHN model with multi-frequency signal.  $T_{e1} = 20$ ,  $T_{e2} = 30$ ,  $\varphi = 0$ ,  $A = 0.085$ . ISIH of the mean field of various systems, (b) from left to right  $N = 3, 30, 700$ .  $T_{e1} = 20$ ,  $T_{e2} = 30$ ,  $\varphi = 0$ ,  $A = 0.085$ ,  $D = 10^{-6}$ , (c) from left to right  $N = 3, 80, 500$ .  $T_{e1} = 20$ ,  $T_{e2} = 30$ ,  $\varphi = e(2.718...)$ ,  $A = 0.084$ ,  $D = 10^{-8}$ , (d) from left to right  $N = 3, 60, 500$ .  $T_{e1} = 20$ ,  $T_{e2} = 5$ ,  $\varphi = 0$ ,  $A = 0.0726$ ,  $D = 10^{-6}$ . The threshold for identifying a spike is 1.0.

this question by replacing the signal term in eqn (2) with  $A\left(\sin\left(\frac{2\pi}{T_{e1}}t\right) + \sin\left(\frac{2\pi}{T_{e2}}(t + \varphi)\right)\right)$ . To understand in detail the response of a single FHN model or coupled system to multi-frequency signal and noise is a challenging task; we just want to show here that by varying the system size  $N$ , one can achieve selective response to a multi-frequency signal. We think this is a promising mechanism in living organisms. Some exemplary results are shown in Fig. 4. When considering a single model with  $T_{e1} = 20$ ,  $T_{e2} = 30$ ,  $\varphi = 0$ ,  $A = 0.085$ , the curve of output coherence  $R$  vs. noise amplitude  $D$  (Fig. 4a) shows triple local minima. The ratio of the largest resonant  $D$  to smallest resonant  $D$  in Fig. 4a is  $10^9$ , so it's too time-consuming to get the corresponding curve of  $R$  vs.  $N$  as is the case of Fig. 1 and Fig. 2 because the maximal system size  $N$  for a complete curve is too large for a personal computer. We choose a smaller noise amplitude  $D = 10^{-6}$  then vary  $N$ , and display in Fig. 4b some typical ISIH to demonstrate frequency-selective response of the mean field. With certain large size, the mean field fires with the least common multiple ( $T_{lcm}$ ) of the two external periods (right). With a certain intermediate system size, the firing pattern is a spectrum of  $T_i$ ,  $T_{e1}$ ,  $T_{e2}$ , and  $T_{lcm}$  (middle). Further decreasing the system size,  $T_{lcm}$ , as a component in the spectrum, disappears (left). With a larger noise amplitude  $D$  and very small system size, the external signal is overwhelmed and only  $T_i$  is manifested (this case not shown). Actually, the details of the response pattern are closely dependent on signal periods and the phase. For parameters different from those considered above, the firing pattern is different. However, the phenomenon of selective response due to varying system size is ubiquitous. We show two firing patterns that are more complex in Fig. 4c and d. In Fig. 4c, we have considered an irrational phase  $\varphi = e(2.718\dots)$ ,  $T_{e1} = 20$ ,  $T_{e2} = 30$ , other parameters are  $A = 0.084$ ,  $D = 10^{-8}$ . The spectra of firing patterns have more components than in the case of  $\varphi = 0$ . Some harmonics of  $T_{e1}(20)$ , 80 and 100, appear; while harmonics of  $T_{e2}(30)$  except for  $T_{lcm}$  do not appear. Selective response to  $T_{lcm}$  is also present, but is different from the case of  $\varphi = 0$ . The component  $T = 36$  other than  $T_{lcm}$  is preferred in the case of larger system size. We have also investigated other phases, for example  $\varphi = e^2$ ,  $e^3$ ,  $e^4$ ,  $2e$ ,  $3e$ ,  $\pi/7$ , and  $\pi/11$ , the firing pattern is either the same as of  $\varphi = 0$  or as of  $\varphi = e$ . In Fig. 4d, we have investigated the case of incommensurable periods:  $T_{e1} = 20$ ,  $T_{e2} = 5\pi$ ,  $\varphi = 0$ ,  $A = 0.0726$ ,  $D = 10^{-6}$ . In contrast to the case of commensurable periods, one cannot observe accurate base or higher harmonics of  $T_{e1}$  or  $T_{e2}$  in the responses. Instead, spectrum components nearly to be the common multiples of  $T_{e1}$  and  $T_{e2}$  are found. For instance, response with  $T = 62$  is close to the 4th harmonic of  $T_{e1}$  and the 3rd harmonic of  $T_{e2}$ , as shown in the fourth column of Table 1. In this case, different nearly common multiples are selected by the system size; the smaller the system size, the shorter periods are selected.

In this paper, we have shown that in the presence of a subthreshold signal and noise, the spikes of the mean field of system of globally coupled FHN models can be organized according to the time-scale of the signal, or to the intrinsic time-scale of the FHN model itself, or to the hybrid of the two, by choosing properly the system size. If the external signal is multi-frequency, the effect of frequency-selective response *via* system size multi-resonance is present. The least-common-multiple periods or other common multiples could be selected by different system sizes.

**Table 1** Comparison the harmonics of external signals with the components of response spectrum

Harmonics of $T_{e1}$ ( $5\pi$ )	15.7	31.4	47.1	62.8	78.5
Harmonics of $T_{e2}$ (20)	20		40	60	80
Responses as nearly common multiple	17		44	62	79

Recently, much attention has been paid to frequency-encoded signals in a biological context. For example, Hajnoczky *et al.* have studied the control of  $\text{Ca}^{2+}$ -sensitive mitochondrial dehydrogenases (CSMDHs) with cytosolic  $\text{Ca}^{2+}$ .<sup>23</sup> They conclude that the frequency of cytosolic  $\text{Ca}^{2+}$  oscillations can control the CSMDHs over the full range of potential activities. Dolmetsch *et al.* demonstrated that the frequency of cytosolic  $\text{Ca}^{2+}$  oscillations could differentially control the activation of distinct sets of transcription factors and the expression of different genes.<sup>24</sup> Li *et al.* showed that the oscillations in cytosolic free calcium levels at roughly physiological rates could maximize gene expression.<sup>25</sup> The frequencies in their experiments are artificial; however, results in this paper present a practically potential mechanism that could be employed by living organisms to modulate biological oscillation frequencies. The feature in Fig. 4b and d, larger size preferring longer period, reminds us of the relation between ultradian rhythms, which result from activities at the cellular level, and the size of the organisms.<sup>26</sup> If we compare the main idea of the system size resonance, which is manifested in dynamical equations mainly by an additional term proportional to  $D/\sqrt{N}$ , with the form of the chemical Langevin equation,<sup>27</sup> we can reasonably regard the number of molecules that are involved in cellular processes as the system size considered in this paper. Therefore, the results in this paper may find application in the determination of characteristic frequencies in cellular processes and in the explanation of the optimal size of organisms. On the other hand, in the biological context of information detection and transmission, the results in this paper provide a possibility for selective function by varying the size of the operating system.

## Acknowledgements

This work is supported by the National Science Foundation of China (20203017, 20433050), and the Foundation for the Author of National Excellent Doctorial Dissertation of PR China (FANEDD).

## References

- L. Gammaitoni, P. Hanggi, P. Jung and F. Marchesoni, *Rev. Mod. Phys.*, 1998, **70**, 223.
- B. Lindner, J. Garcia-Ojalvo, A. Neiman and L. Schimansky-Geier, *Phys. Rep.*, 2004, **392**, 321.
- K. Miyakawa and H. Isikawa, *Phys. Rev. E*, 2002, **65**, 056206.
- Z. Hou, L. Yang, X. Zuo and H. Xin, *Phys. Rev. Lett.*, 1998, **81**, 2854.
- Z. Hou and H. Xin, *Phys. Rev. Lett.*, 2002, **89**, 280601.
- P. Hanggi, *ChemPhysChem*, 2002, **3**, 285.
- J. K. Douglas, L. Wakens, E. Pantazelou and F. Moss, *Nature*, 1993, **365**, 337.
- J. E. Levin and J. P. Miller, *Nature*, 1996, **380**, 165.
- J. J. Collins, T. T. Imhoff and P. Grigg, *J. Neurophysiol.*, 1996, **76**, 642.
- B. J. Gluckman, T. I. Netoff, E. J. Neel, W. L. Ditto, M. L. Spano and S. J. Schiff, *Phys. Rev. Lett.*, 1996, **77**, 4098.
- E. Manjarrez, J. G. Rojas-Piloni, I. Mendez, L. Martínez, D. Vélez, D. Vázquez and A. Flores, *Neurosci. Lett.*, 2002, **326**, 93.
- D. F. Russel, L. A. Wilkens and F. Moss, *Nature*, 1999, **402**, 291.
- L. Gammaitoni, F. Marchesoni and S. Santucci, *Phys. Rev. Lett.*, 1995, **74**, 1052.
- (a) A. Longtin and D. R. Chialvo, *Phys. Rev. Lett.*, 1998, **81**, 4012; (b) S. R. Massanes and C. J. Perez Vicente, *Phys. Rev. E*, 1999, **59**, 4490.
- A. S. Pikovsky and J. Kurths, *Phys. Rev. Lett.*, 1997, **78**, 775.
- (a) J. J. Collins, C. C. Chow and T. T. Imhoff, *Nature*, 1995, **376**, 236; (b) J. F. Lindner, B. K. Meadows and W. L. Ditto *et al.*, *Phys. Rev. Lett.*, 1995, **75**, 3; (c) J. F. Lindner, B. K. Meadows, W. L. Ditto, M. E. Inchiosa and A. R. Bulsara, *Phys. Rev. E*, 1996, **53**, 2081.
- Z. Gao, B. Hu and G. Hu, *Phys. Rev. E*, 2001, **65**, 016209.
- J. F. Lindner, J. Mason, J. Neff, B. J. Breen, W. L. Ditto and A. R. Bulsara, *Phys. Rev. E*, 2001, **63**, 041107.

- 19 (a) A. Pikovsky and A. Zaikin, *Phys. Rev. Lett.*, 2002, **88**, 050601;  
(b) R. Toral, C. R. Mirasso and J. D. Gunton, *Europhys. Lett.*,  
2003, **61**(2), 162.
- 20 E. I. Volkov, E. Ullner, A. Zaikin and J. Kurths, *Phys. Rev. E*,  
2003, **68**, 026214.
- 21 G. Escalera, M. Rivera and P. Parmananda, *Phys. Rev. Lett.*, **92**,  
230601.
- 22 D. J. Higham, *SIAM Rev.*, 2001, **43**(3), 525.
- 23 G. Hajnoczky, L. Robb-Gaspers, M. Seitz and A. P. Thomas,  
*Cell*, 1995, **82**, 415.
- 24 R. Dolmetsch, K. Xu and R. Lewis, *Nature*, 1998, **392**, 933.
- 25 W. Li, J. Liopis, M. Whitney, G. Zlokarnik and R. Y. Tsien,  
*Nature*, 1998, **392**, 936.
- 26 B. Smith, *Moving 'Em: A Guide to Low Stress Animal Handling'*,  
Graziers Hui, Kamuela, HI, 1998, p. 37.
- 27 D. Gillespie, *J. Chem. Phys.*, 2000, **113**, 297.